Chapter 5

# Friction Stir Welding of Aluminium Alloys

Rajkumar Vijayakumar, Venkatesh Kannan and
Arivazhagan Natarajan

Additional information is available at the end of the chapter

http://dx.doi.org/10.5772/intechopen.70233

**Abstract**

This chapter investigates on the characterization of friction stir welded dissimilar aluminium alloys AA2024 with AA5052, AA2024 with AA6061 and AA 5052 with AA6061. Five tool designs were employed with first two dissimilar combinations to analyze the influence of rotation and traverse speed over microstructural and mechanical properties. H13 tool steel was used as tool material with various pin profiles which includes cylindrical, cylindrical-threaded, squared, tapered and stepped types. In the dissimilar welding of AA 2024 with AA 5052, sound welds were produced with stepped pin tool. In the dissimilar welding of AA 2024 with AA 6061, ratio between tool shoulder to diameter of tool pin was the most influential factor. Welded joints failed in the Heat affected zone (HAZ) of 6061 where the hardness values were comparatively less. In dissimilar welding of AA 5052 with AA6061, cylindrical pin tool was used at a constant speed of 710 rpm and at different feed rates of 28 and 40 mm/min. Micro structural examination showed variation of grain size in every zone and their influence on mechanical properties. Correlating mechanical and metallurgical properties, the optimized process parameters of speed and feed were identified to be 710 rpm and 28 mm/min respectively for all attempted dissimilar combinations.

**Keywords:** aluminium alloy, friction stir welding, dissimilar welding, AA2024, AA 5052, AA6061

## 1. Introduction

Aluminium alloys are widely used in variety of applications ranging from basic to complex such as in the making of aircraft bodies. Due to varied service conditions, there are scenarios where different series of aluminium alloys are to be joined. The most extensively used non precipitation hardenable series of Al alloys in aeronautical applications are 3xxx, 5xxx. Some of the precipitation hardenable series of Al alloys include 2xxx, 6xxx and 7xxx series. Merits of 2xxx series are that they possess excellent mechanical properties at high temperatures whereas 7xxx series show good mechanical properties at low temperatures and also exhibit high corrosion resistance properties [1]. Identification of appropriate joining process and process parameters employed becomes important in service performance of these materials and in its actual service conditions. aluminium alloys are lighter yet possess good strength and ductility. This makes the material a preferable candidate to work in varied working environments.

AA2024, AA5052 aluminium alloys are widely used in, automotive, aerospace and shipbuilding industries [2]. Fusion welding of dissimilar aluminium alloys is very challenging mainly due to the formation of low melting eutectics by the constituent elements resulting in weld solidification cracking. Hot cracking in aluminium alloys are extremely sensitive to weld metal compositions [3]. Hence solid state joining process becomes more suitable for welding aluminium alloys, since this process does not involve melting. Hence the defects like weld solidification cracking, porosity, segregation, liquid cracking on heat effected zone and brittle inter metallic formation could be avoided using this technique [2, 4]. In FS welding techniques, tool geometry plays a major role in obtaining desirable metallurgical and mechanical properties [5–7].

In this study AA2024 and AA5052 were fabricated using friction stir welding process using five different tool pin profiles. Four traditional pin profiles namely cylindrical, threaded, squared, tapered pin and a newly designed stepped pin profile were employed in this research. Al-Cu dissimilar metals were welded as in reference [4] and found that better tensile strengths were achieved in the plates which was welded at 710 rpm, where the tested speed range was 600–1000 rpm. They also concluded that the defect-free joints could be obtained when the plates that had superior mechanical properties were fixed on the advancing side. The author reported that the pin transfers the material layer by layer, while the shoulder transfers the material in bulk and forges it. FS welding of AA 6061 has experimented as in reference [8] by changing ratio of shoulder to pin diameter and reported that the defect free welding can be obtained when keeping the D/d ratio is 3:1. Studies on the FS welding of AA 2219-AA5083 alloy as in reference [3] by changing various pin profiles and found that, cylindrical threaded pin has produced defect free welding with good tensile strength. From extensive literature survey it can be deduced that the newly developed stepped pin profile has not been incorporated in the friction stir welding of aluminium alloys.

Aluminium alloy AA6061, is extensively used in marine industries and in the construction of storage tanks and pipelines. Joining process for dissimilar materials are considered quite challenging as compared to joining similar metals, due to change in chemical composition of base metals and their mechanical properties [9–11]. Fusion welding of nonferrous metals is tedious due to high heat inputs. Formation of secondary phase in friction stir welding (FSW) process is absent since the temperature reached in this process is well below the melting point of parent metals.

Thermal dissipation emanates local isothermal stresses. This thermal gradient developed has important and adverse effect on the metallurgical properties and in turn on the mechanical properties of the joint, precisely in the formation of soft zones. This microstructural change affects the performance in service conditions of the weld joints, since mechanical properties decreases with reference to the base material. Valuable details can be obtained by understanding weld thermal cycles precisely in conjunction with transformation curves and their microstructural effect in mechanical properties [12].

Literatures indicate that optimal parameters for joining of dissimilar aluminium alloys are rotation speeds being 600–1000 rpm, D/d ratio of 3:1 traverse speeds around 15–40 mm/min. Out of many materials processed using FSW, the most commendable results obtained were for aluminium and all of its alloys including cast and wrought conditions. Most influential parameters in the FSW process were researched to be tool geometry, travel speed, rotational speed, rotational direction, rotational axis, eccentricity [13]. Studies show that out of two base metals employed, when harder material is placed on the advancing side and softer material in retreating side, better mechanical properties are obtained. Different tool profiles are investigated by researchers, as geometry of tool pin plays a major role in FSW. Threaded, squared and triangular tool pin profiles are efficient to transfer the material from top to bottom of the joint and vice versa by stirring action. The analysis of the results during certain experiments by researchers revealed that during the time of mechanical tests performed, the crack initiation may be significant, at least for welded joints with relative lower stress concentrations and low to moderate loads [14]. Certain researchers have attempted various welding techniques on aluminium alloys. Gas metal arc welding (GMAW), shielded metal arc welding (SMAW) and gas tungsten arc (GTA) welds have been attempted for welding aluminium alloys. Important morphological characteristics have been observed on MIEW process when compared to that of GMA welds. When MIEW welds were fabricated, solidification process tended to promote heterogeneous nucleation. Therefore, auto refinement of grain size is promoted. On the other hand, when multi pass GMA welds were employed, columnar epitaxial solidification happens resulting in increase in grain size [15, 16].

Aluminium alloys AA 5052 and AA 6061 are FS welded with specific tool contours and using two welding parameters of variable feed rate and constant speed. This chapter also discusses on characterization of metallurgical and mechanical properties of the above combination to evaluate the performance characteristics of FS welded joints.

## 2. Experiments and procedures

### 2.1. Materials and methods

The materials used in this study are commercially available AA 2024-T4 (Al-Cu alloy), AA 5052 and AA 6061-T4 (Al-Mg-Si alloy). Plates of 5 mm thick AA2024, AA5052 and AA6061 were friction stir welded in certain combinations using conventional milling machine employing a specially designed fixture. The chemical compositions of the samples are tabulated in **Table 1**.

D/d ratio (shoulder/pin) was kept as 3, where shoulder diameter is 16 mm and pin diameter being 6 mm. The aluminium plates were made into coupons of 100 mm × 50 mm where the welding was carried out using milling machine with necessary fixtures. AISI H13 tool steel which has high thermal fatigue resistance was used in this study.

| Material | Mg | Mn | Cu | Fe | Si | Cr | Zn | Ti | Al | % of Elongation |
|---|---|---|---|---|---|---|---|---|---|---|
| AA2024 | 1.5 | 0.6 | 4.35 | 0.5 | 0.5 | 0.10 | 0.25 | 0.15 | Rem | 137 |
| AA5052 | 1.4 | 0.14 | 0.14 | 0.4 | 0.26 | 0.15 | 0.08 | – | Rem | 330 |
| AA6061 | 1 | 0.15 | 0.27 | 0.7 | 0.6 | 0.19 | 0.6 | 0.15 | Rem | 75 |

**Table 1.** Chemical composition of base metals.

### 2.2. Mechanical characterization

Tensile test was carried out using INSTRON 8801 UTM according to ASTM E8/E8M standards of sub size specimen and the tests were carried out at a strain rate of 0.5 mm/min. Micro hardness measurements were carried out at a load of 100 gf with dwell time of 10 s and distance of 0.25 mm interval across the weldment.

### 2.3. Microstructural characterization

To study the microstructure of the weldments of these dissimilar aluminium alloys Keller's reagent (150 ml water + 3 ml of Nitric Acid, 6 ml of hydrochloric and hydrofluoric acid) was used. In order to analyze the constituents in thermo-mechanically affected zone (TMAZ) and weld, scanning electron microscopy (SEM) with energy-dispersive spectroscopy (EDS) was used.

### 2.4. Process parameters

In dissimilar welding of AA2024 with AA 5052 and AA 2024-T4 (Al-Cu alloy) with AA 6061-T4 (Al-Mg-Si alloy) welding was carried out by placing AA2024 in the advancing side. It was due to higher mechanical strength of AA 2024. AA 5052 and AA6061 were placed on the retreating side. Different pin profiles viz. cylindrical, threaded, squared, tapered and stepped pin were used in this study. The length of tool pin is kept constant at 4.8 mm. Experiments were conducted at a feed rate of 40 mm/min and 28 mm/min against two different speeds of 710, 1000 rpm. The tensile test results welded with all tool profiles and their Ultimate tensile strength (UTS) values along with place of fracture is tabulated in **Table 2**.

The process parameters used in the welding of AA 2024-T4 (Al-Cu alloy) and AA 6061-T4 (Al-Mg-Si alloy) is given in **Table 3**.

| S No | Tool pin profile | UTS (MPa) | Percentage strength | Fracture spot |
|---|---|---|---|---|
| 1 | Threaded | 259 | 78 | TMAZ of 5052 |
| 2 | Squared | 200 | 60 | Weld |
| 3 | Stepped | 297 | 90 | TMAZ of 5052 |
| 4 | Cylindrical | 195 | 59 | Weld |
| 5 | Tapered | 202 | 61 | Weld |

**Table 2.** Tensile test results of AA 2024 and AA 5052 welded specimens.

| S No | Tool design | Rotational speed | Traverse speed (mm/min) | Tilting angle (deg) |
|---|---|---|---|---|
| 1 | Threaded pin | 710 and 1000 rpm | 28 | 2 |
| 2 | | | 40 | |
| 3 | Squared pin | 710 and 1000 rpm | 28 | |
| 4 | | | 40 | |
| 5 | Tapered pin | 710 and 1000 rpm | 28 | |
| 6 | | | 40 | |
| 7 | Cylindrical pin | 710 and 1000 rpm | 28 | |
| 8 | | | 40 | |
| 9 | Stepped pin | 710 and 1000 rpm | 28 | |
| 10 | | | 40 | |

**Table 3.** Welding parameters of AA 2024 and AA 5052 alloys.

The dissimilar alloys AA 5052 and AA6061 were butt welded using cylindrical pin tool with 2 threads. AA 5052 was kept at the advancing side and AA6061 in the retreating side. The two specimens were welded using two parameters: 710 rpm at 28 mm/min and 710 rpm at 20 mm/min.

## 3. Results and discussion

### 3.1. Dissimilar friction stir welding of AA 2024 - AA5052 alloys

#### *3.1.1. Metallurgical characterization*

The different types of pin profiles used in this work along with the corresponding tool dimensions can be seen from **Figure 1**(**a**–**e**).

It is observed that macroscopic defects appeared when using the cylindrical pin tool. The cross sectional macrograph is represented in **Figure 2**(**a**–**e**).

It clearly shows void defect while using cylindrical and tapered pin tool. This could be due to inferior metal flow during the welding process while using the corresponding profile tools. On the other hand, the joints fabricated using threaded, squared and stepped pin appeared to be free from defects which could possibly be due to effective mix-up and proper inter diffusion of elements from both base metals. It could also be due to optimized heat input within the weld nugget while using these profiled tools. This may be due to lack of heat input during the welding process and the nature of pin profile. Comparing all tool pin profiles, threaded pin and stepped pin resulted in uniform mix-up of elements from both base metals. The micrographs of FS welded samples obtained using these tool profiles are represented in **Figure 3**(**a**–**f**).

It is observable from **Figure 3**(**a** and **d**) that the material flow from advancing side of AA2024 to the weld nugget is vivid in both threaded and stepped pin profiles. Further refined grain structures appeared on the weld nugget as well as on the AA2024 side.

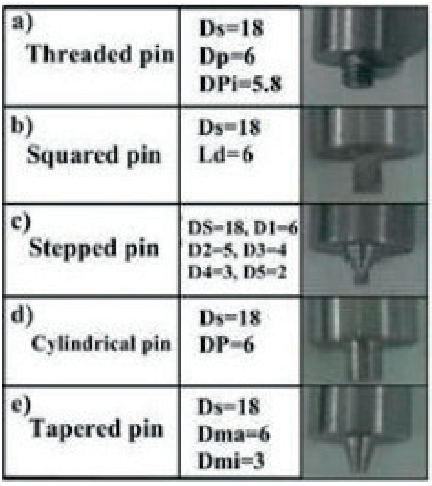


**Figure 1.** Various tool pin profiles used and their dimensions.

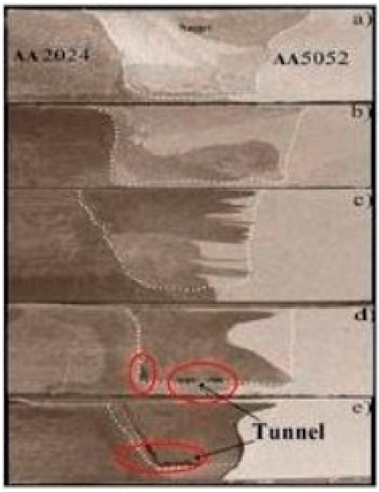


**Figure 2.** Cross sectional macrostructures of welded samples.

*3.1.2. Mechanical characterization*

The tensile test has been carried out for the FS welded samples and the averaged results are represented in **Table 2**. Two samples were tested on weldments fabricated with each tool pin profiles to ensure the repeatability of weld consistency and testing. Samples welded with threaded pin gave tensile strength of 259 MPa which is 78% of the strength of AA5052. Interestingly the stepped pin profile yielded tensile strength of 297 MPa. The fracture also occurred at the TMAZ of AA5052 and not in the weld. Squared pin, cylindrical pin, and tapered pin fractured in nugget with 60, 59, and 61 percentage of base strength of AA 5052. Stress-strain graphs plotted for both samples are depicted in **Figure 4**.

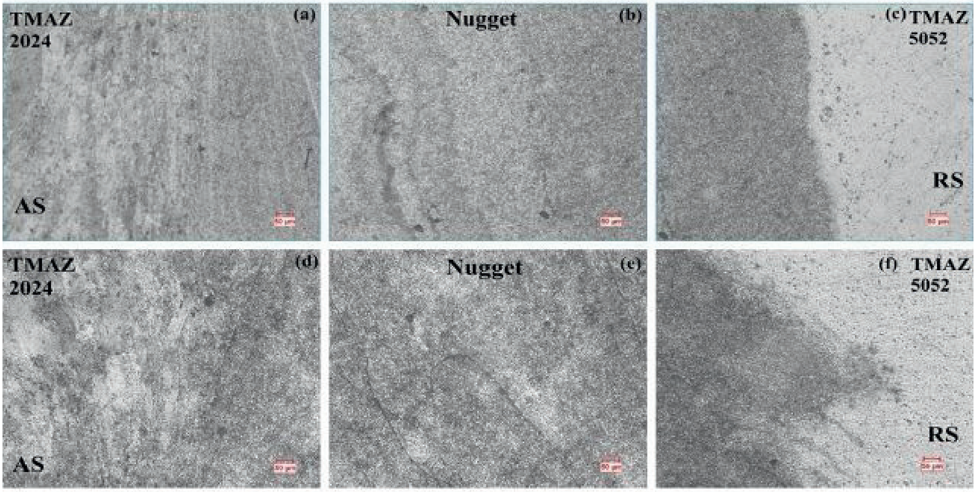


**Figure 3.** Microstructures captured at various zones of AA 2024 and AA5052 welds.

The hardness profiles of the samples welded with traditional tool pins were found to have lower range of hardness value in the weld nugget and heat affected zone. In both the cases, it is apparent the hardness values in the weld nugget seems to be higher than that of the base metal of AA 5052 and less that of AA2024. Hardness plot for threaded and stepped pin profile weldments can be seen from **Figure 5**.

Sudden drop in the hardness value from weld zone to TMAZ in retreating side led to the fracture at that point as micro hardness values are directly proportional to the strength of weld which is also evident from the tensile test. The hardness profile noticed in the weld region of the sample welded with stepped pin is comparatively higher than that of the hardness achieved in

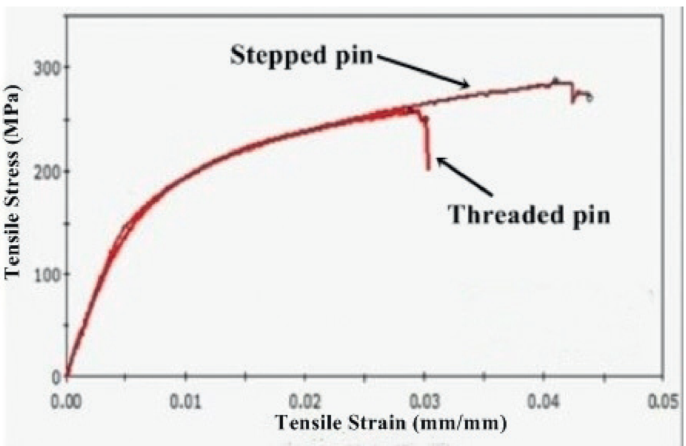


**Figure 4.** Stress strain plots of AA 2024 and AA 5052 welded samples.

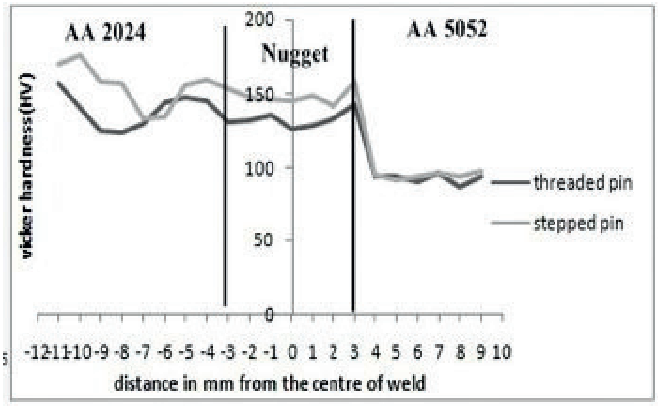


**Figure 5.** Hardness plots of threaded and stepped pin welded samples.

joints obtained using other tool profiles eventually proving high strength. Average micro-hardness value of 150 HV was obtained in the welded joints produced through stepped pin tool.

### 3.2. Dissimilar friction stir welding of AA2024-AA6061 alloys

The surface morphologies of the weld fabricated using cylindrical, threaded and squared pin tool profile are shown in **Figure 6**(**a** and **b**).

The traverse speed and rotational speed for threaded and squared pin were fixed at 28 mm/min at 710 rpm and 40 mm/min at 1000 rpm for respective samples. By varying the process parameters and tool geometry, no defects were found in the welds except for tapered pin. Defective surface morphologies and improper heat diffusion were observed on using tapered pin (**Figure 6(b)**).

#### *3.2.1. Macrostructures*

From the macro-graphic studies, different regions of weldments are identified and it represents the effective stir of both the base material in the nugget zone **Figure 6**(**c**, **d**).

The presence of AA2024 constituent elements in the nugget is more when compared to AA6061. This is because AA2024 was placed on advancing side of the weld. Welds without voids were fabricated using cylindrical threaded pin with parameters of 710 rpm, 28 mm/min and using squared pin with parameters of 1000 rpm, 40 mm/min. For the same process parameters, few macroscopic defects occurred on using cylindrical, tapered and stepped pin. This could be attributed to absence of vertical traverse of metal in nugget region.

#### *3.2.2. Microstructural analysis*

The microstructures at different regions of the welded dissimilar materials are shown in **Figure 7**(**a–g**).

There are no substantial changes in the base metal microstructure, though the weld nugget undergoes considerable amount of thermal changes. It is evident from the microstructure

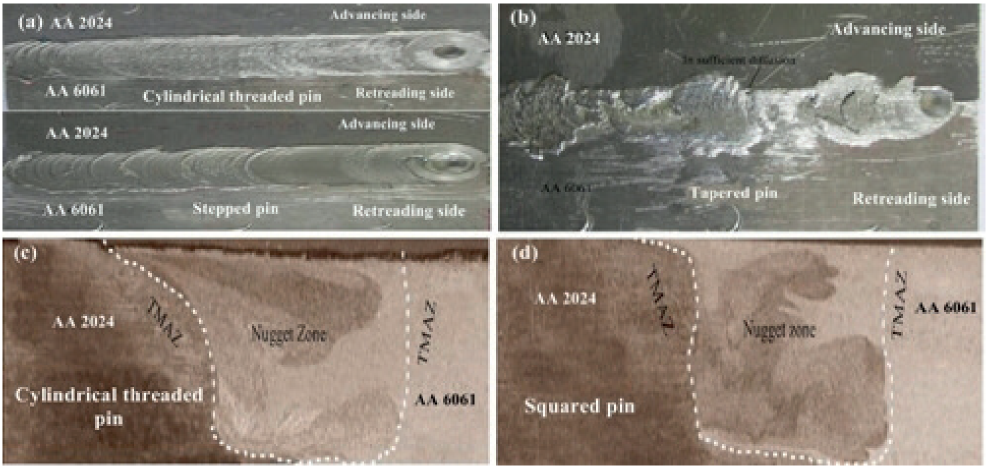


**Figure 6.** Surface morphology of AA2024 and 6061 welds and macrographs of threaded and squared pin profiles.

(**Figure 7**(**b** and **f**)) that the thermal cycle has significantly influenced the heat affected zone. Yet there is no plastic deformation occurred in this region. There is considerable grain growth in the thermo-mechanically affected zone (TMAZ). This could be due to the plastic deformation and low heat levels encountered during welding. A distinct boundary separates the recrystallized zone (weld nugget) from the TMAZ, which is apparent from the micrographs. The dynamically recrystallized zone is the stirred zone. Severe plastic deformation has taken place in this zone resulting in fine equiaxed grains. Stirred zone is a commonly used phrase in friction stir processing which denotes that substantial volume of material is being processed. Weld nugget micrographs (**Figure 7(d)**), depicts highly refined and increased grain boundaries, which has enhanced the weldment strength.

*3.2.3. Tensile test*

Maximum weld strength of 194 MPa and 209 MPa were obtained for cylindrical threaded and squared pin, respectively. As shown in **Figure 8**, for both the tool pin geometries, fracture occurred at the HAZ of 6061 alloy.

For the other tool pin geometry fracture has occurred at the stirred zone. The weld region shows lower strength compared to both base metals. Joint efficiencies obtained for cylindrical threaded pin and squared pin are 80 and 87%, respectively.

*3.2.4. Hardness measurements*

Vickers hardness tests were conducted across the various regions of the weld spacing of (0.25 mm) shown in **Figure 9**.

Average hardness value across the weldments obtained for cylindrical threaded pin and for squared pin were 105.15 HV and 135.6 HV respectively. The hardness of weld nugget was considerably less than that of AA2024, whereas the hardness was comparatively higher than base metal of 6061 and TMAZ.

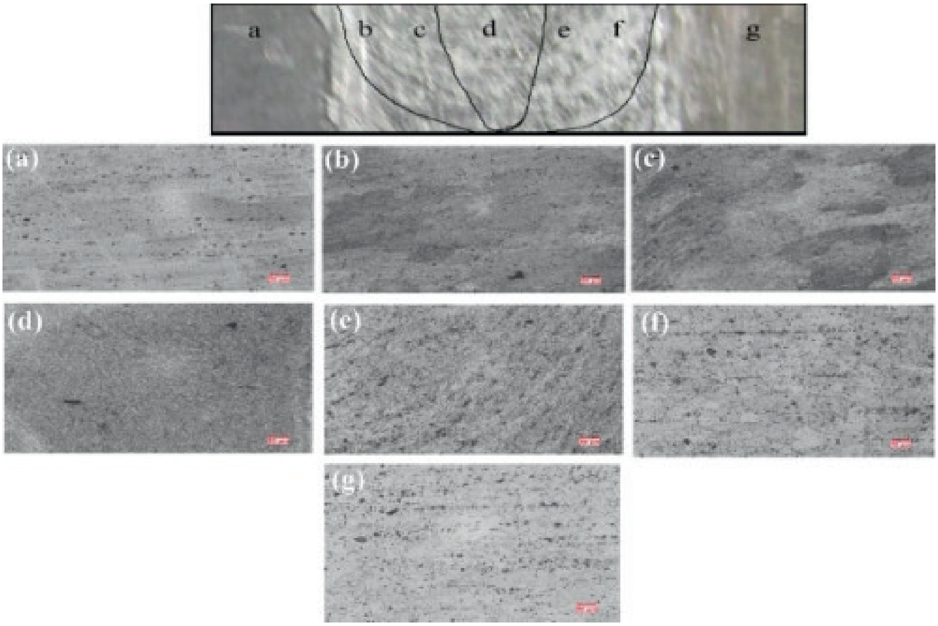


**Figure 7.** Microstructures captured at various zones of AA 2024 and AA 6061 weldment.

## 3.3. Dissimilar friction stir welding of AA 5052 and AA 6061 alloys

Evolution of grain structures, their texture, temperature gradient, recrystallization techniques and precipitation of inter – metallic constituents are some of the factors included in micro structural studies. These factors indeed influence the quality and strength of any welds when

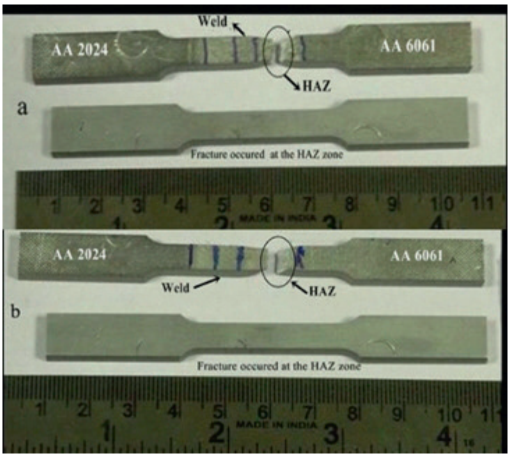


**Figure 8.** Tensile tested AA 2024 and AA 6061 samples welded with (a)Cylindrical threaded pin (b) Squared pin.

http://dx.doi.org/10.5772/intechopen.70233

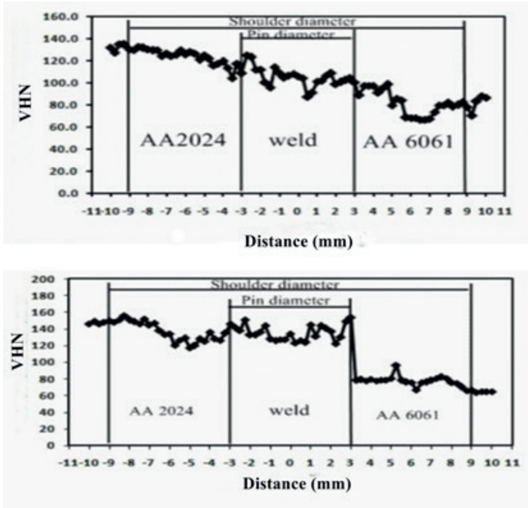


**Figure 9.** Hardness plots of samples welded using threaded and stepped pin profiles.

assessed through tests namely tensile, creep, fatigue etc. [17]. The tool dimension and the tool used for welding are shown in **Figure 10**(**a** and **b**).

*3.3.1. Cross sectional macrographs*

The cross sectional macrograph of weldments showed proper material flow from advancing side to retreating side. This is evidence of the fact that the weld process parameters considered are optimal. A micro void was visible in the sample welded at 40 mm/min (**Figure 10(d)**). This may be due to improper fusion involved in the weld nugget.

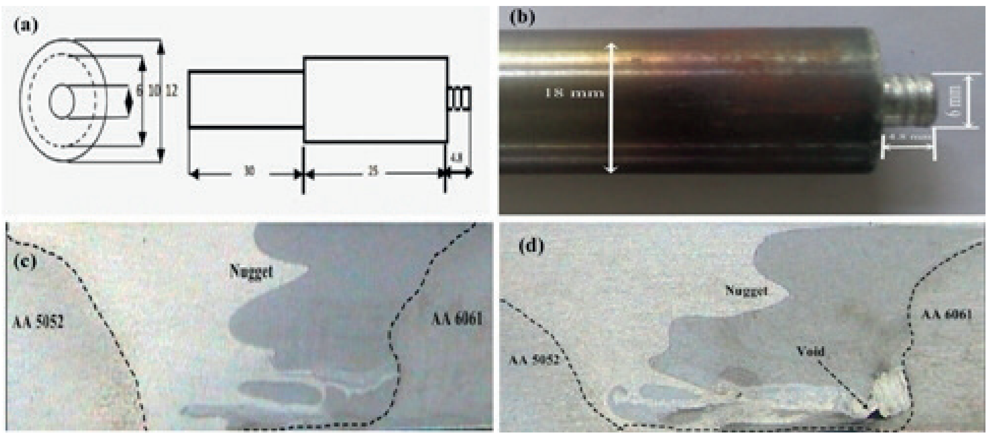


**Figure 10.** Dimensions of cylindrical threaded tool pin and cross sectional macrostructures of welded samples.

### *3.3.2. Microstructural analysis*

The microstructures taken at various regions of the weldments of both the samples are shown in **Figure 11**.

The microstructures of the base metals of AA 5052 and AA 6061 are shown in **Figure 11**(**a** and **b**) respectively, whereas **Figure 11**(**c** and **d**) shows the micrographs at TMAZ. **Figure 12**(**a** and **b**) shows the microstructures of weld region and **Figure 12**(**c** and **d**) depicts the microstructures at the interfaces.

It can be observed from (**Figure 11**(**e** and **f**)) that grain formation is refined in the weld zone as compared to TMAZ of both alloys. This should be due to optimality of process parameter that was selected and effective cooling rate. In addition, on comparing the both TMAZ's, AA 6061 side has considerable grain size increase (**Figure 11(f)**).

This may have led to deterioration of tensile properties in this zone. It has been analysed in reference [6] that the change of grain size is due to the effect of elevated temperatures and that the strain rates were insignificant. It was also concluded that the decrease in the flow stress at high temperatures was primarily due to the thermally activated dislocation lines.

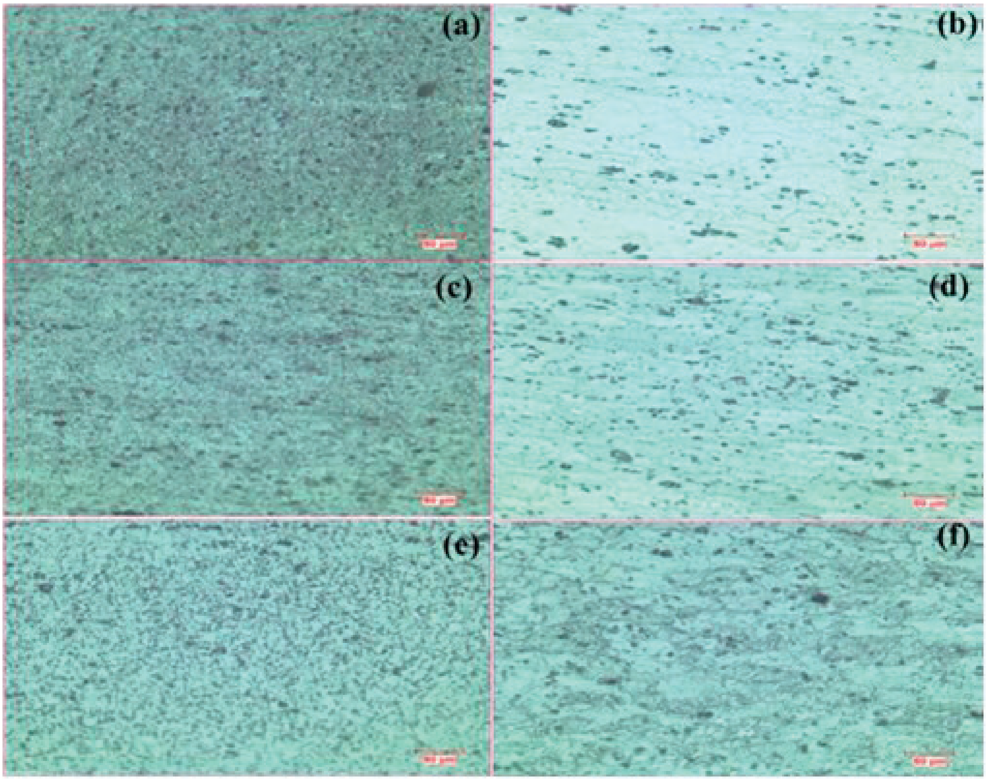


**Figure 11.** Microstructures of AA 5052 and 6061 sample welded at feed rate of 28 mm/min.

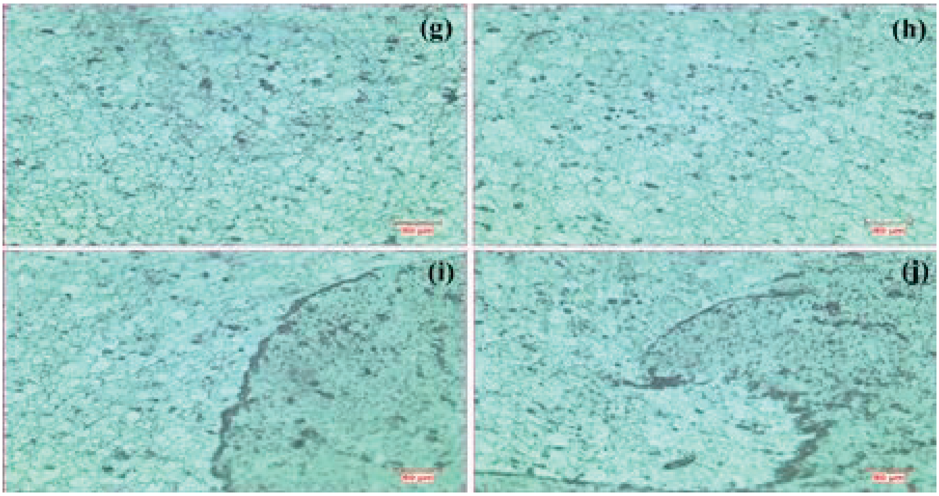


**Figure 12.** Micrographs of AA 5052 and AA 6061 samples captured at (g & h) weld regions and (I & j) at interface regions.

### 3.3.3. *Tensile test*

Tensile samples were wire cut using electrical discharge machining (EDM) and prepared according to the ASTM standards of sub-size dimensions. It is vivid from **Figure 13(a)** that in both cases, the fracture has occurred in the TMAZ of the 6061 alloy. This affirms that the weld nugget possesses better strength than base metals.

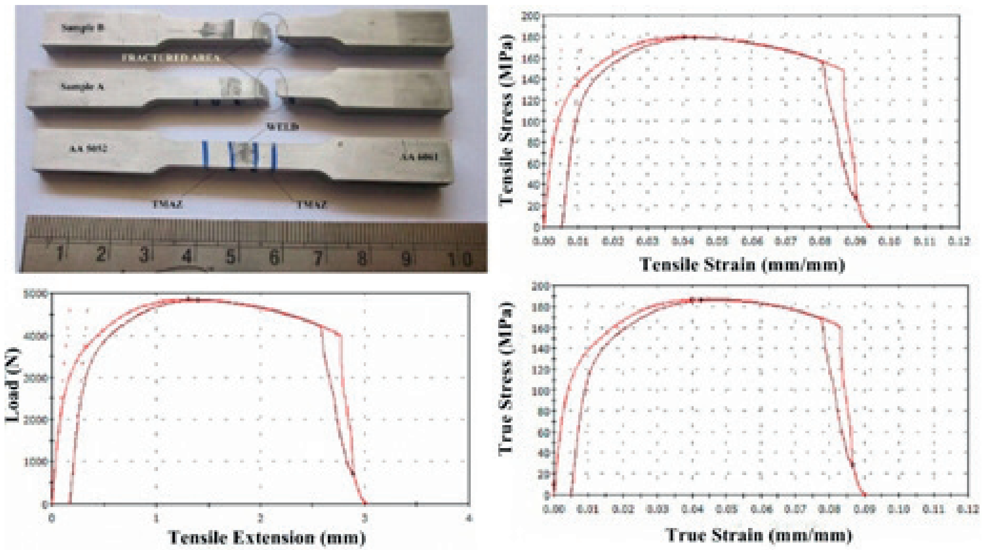


**Figure 13.** Tensile tested specimens and stress strain plots of AA 5052 and 6061 welded specimens.

There is no much difference between UTS of both the samples. However, the tensile stress at break point of Sample B is proportionately higher than Sample A. This means Sample B has yielded suddenly after the elastic limit, whereas Sample A has yielded after demonstrating high ductility. The load at break point adds to the same. Results of tensile test are being tabulated in **Table 4**.

Welding parameters have been optimized as in reference [2] by design of experiments and the optimum level of settings concluded from their experiments. Corresponding parameters chosen for the studies are rotational speed of 700 rpm, transverse speed of 28 mm/min and D/d ratio being 3 respectively. The performance of cylindrical threaded pin tool profile was better among others considered. D/d ratio plays a vital role and contributes to an overall efficiency of about 60%. It is found in reference [17] that the hardness variations in the FS weld zone of Al 5083 alloy could not be supported by study of grain size in the weld region alone. Hence, in any study, correlation of mechanical performances with that of metallurgical factors becomes important in analysing the nature and reason for the fracture.

### *3.3.4. Hardness measurements*

The hardness profile obtained for the samples are shown in **Figure 14**.

From the plots, it can be understood that the feed rate has only little influence on the hardness of the weldments. From the advancing side (AA 5052) to the retreating side (AA 6061) of the weldment, the hardness values show a decreasing trend and again a gradual increasing trend. It is worthy to note that the fracture has also occurred in the TMAZ of AA 6061 (minimum

| Sample | Maximum load | UTS (MPa) | Tensile strain at break (%) | Tensile stress at break (MPa) | Load at break (kN) | Elongation (%) |
|---|---|---|---|---|---|---|
| Sample A | 4853 | 180 | 10.5 | 2.75 | 0.07 | 10.5 |
| Sample B | 4837 | 179 | 8.4 | 27.06 | 0.73 | 8.33 |

**Table 4.** Tensile test report of AA 5052 and AA 6061 welded samples.

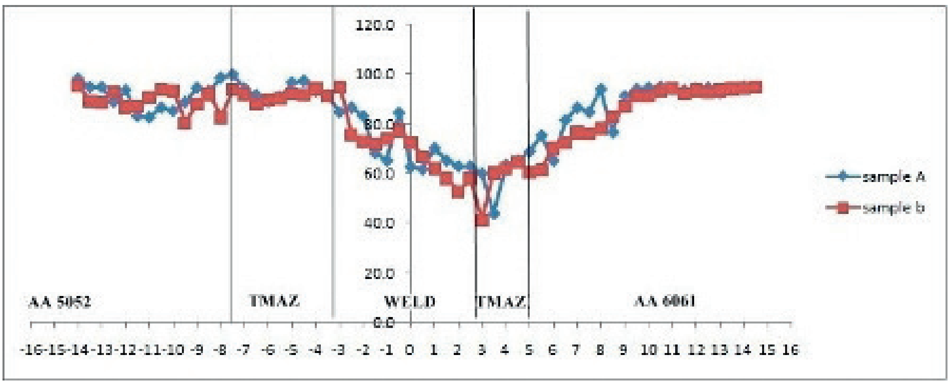


**Figure 14.** Hardness plots of AA 5052 and AA 6061 welded samples.

hardness zone). It can be noted from the graph that hardness values of TMAZ in the retreating side are comparatively less. This could be due to constituent gradient in mixing/diffusion of AA 6061 with material from advancing side and weld nugget. As evident from nature of the micrograph, this could be a reason for the failure of tensile specimen in the TMAZ of AA 6061 side. Moreover, it may be due to the grain coarsening effect that the hardness values in the weld nugget shows lower trend when compared with parent metals.

## 4. Conclusions

- In the FSW of AA 2024 with AA5051, sound welds were produced using a new stepped pin tool, at 710 rpm and 28 mm/min. From morphological studies, there is quantifiable reduction in grain size of weld nugget compared to parent metals. Maximum tensile strength of 297 MPa was achieved on samples welded using stepped pin tool. This strength is comparatively higher than that of the ones that were welded with other profiled pins.
- From the FSW of AA 2024 with AA6061, it is deduced that for cylindrical pin, D/d ratio of 3, rotational speed of 710 rpm, traverse speed of 28 mm/min, were the best optimal parameters. Further, better mechanical properties were observed for the same. In addition, it is concluded that squared pin and cylindrical threaded tool profiles perform better than rest of tool profiles considered.
- FSW between AA 5052 and AA 6061 alloys sounds promising. Cylindrical threaded pin has imparted excellent bondage between both alloys (AA 5052 and AA 6061) by effective FS joining. Both the samples have exhibited nearly equal ultimate strength. In terms of ductility, Sample B (with 710 rpm and 28 mm/min feed rate) outperformed Sample A (with 710 rpm at 40 mm/min).

## Acknowledgements

The authors wish to extend their sincere thanks to SNR Sons Charitable Trust, Coimbatore and the management of VIT University, Vellore for providing necessary support in executing this research.

## Author details

Rajkumar Vijayakumar[1]*, Venkatesh Kannan[2] and Arivazhagan Natarajan[2]

*Address all correspondence to: vrajkumarphd@gmail.com

1 Department of Mechanical Engineering, Sri Ramakrishna Institute of Technology, Coimbatore, India

2 School of Mechanical Engineering, VIT University, Vellore, India

## References


[1] Schneider R, Heine B, Grant RJ. Mechanical behaviour of commercial aluminium wrought alloys at low temperatures. In: Monteiro WA, editor. Light Metal Alloys Applications. Croatia: InTech; 2014. pp. 61-76. DOI: 10.5772/57069

[2] Sheikhi S, Bolfarini C. Preliminary study on the microstructure and mechanical properties of dissimilar friction stir welds in aircraft aluminium alloys 2024-T351 and 6061-T4. Journal of Materials Processing Technology. 2007;**6**:132-142

[3] Koilraj M, Sundareswaran V, Vijayan S, Koteswara Rao SR. Friction stir welding of dissimilar aluminium alloys AA 2219 to AA 5083 – Optimization of process parameters using Taguchi technique. Materials and Design. 2012;**42**:1-7

[4] Xue P, Ni DR, Wang D, Xiao BL, Ma XY. Effect of friction stir welding parameters on the microstructure and mechanical properties of the dissimilar Al-Cu joints. Materials Science and Engineering A. 2011;**528**(13):4683-4689

[5] Li Y, Murr LE, Mcclure JC. Flow visualization and residual microstructures associated with the frictions stir welding of 2024 aluminium to 6061 aluminium. Materials Science and Engineering A. 1999;**271**:213-223

[6] Buffa G, Huaa J, Shivpuri R, Fratini L. Design of the friction stir weld using the continuum based FEM model. Materials Science and Engineering A. 2006;**419**(2):381-388

[7] Mishra RS, Ma ZY. Friction stir welding and processing. Materials Science and Engineering: R: Reports. 2005;**50**(1):1-78

[8] Arora A, Debroy T. Toward optimum friction stir welding tool shoulder diameter. Scripta Materialia. 2011;**64**:9-12

[9] Heidarzadeh A, Khoaverdizadeh H, Mahmoudi A, Nazari E. Tensile behaviour of friction stir welded AA 6061-T4 aluminium alloy joints. Materials and Design. 2012;**37**:166-173

[10] Rao P. Microstructure and mechanical properties of friction stir lap welded aluminium alloy AA 2014. Journal of Materials Science and Technology. 2011;**28**(5):414-426

[11] Kumbhar NT, Sahoo SK, Samajdar I, Dey GK, Bhanumurthy K. Microstructure and micro textural studies of friction stir welded aluminium alloy 5052. Materials and Design. 2011;**32**:1657-1666

[12] Ambriz RR, Jaramillo D. Mechanical behavior of precipitation hardened aluminium alloy welds. In: Monteiro WA, editor. Light Metal Alloys Applications. Croatia: InTech; 2014. pp. 36-59. DOI: 10.5772/58418

[13] Vilica P, Telmo G Santos. Non destructive techniques for detecting imperfections in friction stir welds of aluminium alloys. In: Kvackaj T, editor. Aluminium Alloys Theory and Applications. Croatia: InTech; 2011. pp. 94-114. DOI: 10.5772/14743

[14] Ribeiro AS, de Jesus AMP. Fatigue behaviour of welded joints made of 6061-T651 aluminium alloys. In: Kvackaj T, editor. Aluminium Alloys Theory and Applications. InTech; 2011. pp. 136-156. DOI: 10.5772/14489

[15] Ambriz RR, Mayagoitia V. Welding of aluminium alloys. In: Recent Trends in Processing and Degradation of Aluminium Alloys. Croatia: InTech; 2011. pp. 63-86. DOI: 10.5772/18757

[16] Mahabunphachai S, Koc M. Investigations on forming of aluminium 5052 and 6061 sheet alloys at warm temperatures. Materials and Design. 2010;**31**:2422-2434

[17] Sato Y, Urata M. Hall-Petch relationship in friction stir welds of equal channel angular presses aluminium alloys. Materials Science and Engineering A. 2003;**35**(4):298-305